# Optical directional coupler and Mach-Zehnder interferometer enhanced via 4H-SiC phonons

Michael F. Finch, Claudio A. B. Saunders Filho, Brian A. Lail
Department of Electrical and Computer Engineering, Florida Institute of Technology, 150 West University Blvd., Melbourne, FL 32901, USA
mfinch2009@my.fit.edu, cbarretosaun2014@my.fit.edu, blail@fit.edu

## ABSTRACT

Surface phonon polaritons (SPhPs), similar to it cousin phenomenon surface plasmon polaitons (SPPs), are quasi-neutral particles resulting from light-matter coupling that can provide high modal confinement and long propagation in the mid to long infrared (IR). Mach-Zehnder interferometer (MZI) is a combination of two connected optical directional couplers (ODC). With the use of SPhPs, sub-wavelength feature sizes and modal areas can be achieved and to this end a hybrid SPhP waveguide, where propagation length and modal area can be trade-off, will be employed in the design of an ODC and MZI. This endeavor analyzes and characteristics both an ODC and MZI using commercially available numerical simulation software employing finite element method (FEM). The ODC and MZI are design using a novel SPhP hybrid waveguide design where a 4H-SiC substrate provides the polariton mode. The output ports power and relative phase difference between ports are investigated. SPhP enhanced ODC and MZI has applications including, but not limited to, next-generation ultra-compact photonic integrated circuits and waveguide based IR sensing.

**Keywords:**Surface Phonon Polaritons(SPhP), Mach-Zehnder Interferometer, 4HSilicon Carbide (SiC), Optical Directional Coupler (ODC), Couple Mode Theory (CMT)

## 1. INTRODUCTION

In recent years, a push for minimization of optical and photonic devices has led in advancement and maturing of waveguide technology that exploits ultra-confinement of surface plasmon polaritons (SPPs) in the optical to ultraviolet (UV) spectrum[1,2]. SPPs result from the coupling between the valence electrons in metals and electromagnetic radiations resulting in a transverse magnetic (TM)surface mode at the metal/dielectric interface. Similar in the case of surface phonon polarition (SPhP), a TM surface mode is present, but at a polar dielectric/dielectric interface. The underlying process results from the coupling of the lattice vibrations, phonons, in the polar dielectrics in a band of frequencies where the dielectric permittivity of the polar dielectric becomes negative known as the Reststrahlen band[3,4]. The mathematical treatment for the dispersion relationship for SPhP is similar to that of SPP, and is as follows[1]:

$$k_{SP} = k_0\sqrt{\frac{\varepsilon_m\varepsilon_d}{\varepsilon_m+\varepsilon_d}}, \tag{1}$$

where $\varepsilon_m$ is for metal in the SPP or polar dielectric in SPhP case, $\varepsilon_d$ is the dielectric half space, and $k_0$ is the free space wavenumber. The SPhP hybrid waveguide under consideration is shown in Figure 1at an operating wavelength of 12.4 μm[1,5,6]. The effective refractive index and propagation length can be determined from eq. 1 as the following:

$$n_{sp} = Re\left\{\sqrt{\frac{\varepsilon_m\varepsilon_d}{\varepsilon_m+\varepsilon_d}}\right\}, \tag{2.a}$$

$$L_m = \frac{1}{2Im\{k_{SP}\}}. \tag{2.b}$$

With the use of coupled-mode theory (CMT)[1,7-9], the hybrid mode can be described as a superposition of two uncoupled modes; a waveguide tracer mode and SPhP TM mode. Therefore, a modal character can be defined as:

$$|a|^2 = \frac{n_{hyb}-n_{SP}}{(n_{hyb}-n_{WG})+(n_{hyb}-n_{SP})}, \tag{3}$$

Metamaterials, Metadevices, and Metasystems 2016, edited by Nader Engheta, Mikhail A. Noginov, Nikolay I. Zheludev, Proc. of SPIE Vol. 9918, 99181M

where $n_{sp}$ describes the pure TM polariton surface mode, $n_{WG}$ is the waveguide tracer mode, and $n_{hyb}$ is the resulting hybrid waveguide mode. Here mode character ranges from 0 to 1 where 0 is for pure TM surface mode and 1 is for waveguide tracer mode.

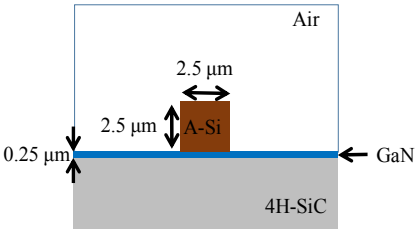


Figure 1. Design hybrid SPhP enhanced waveguide cross-section under consideration.

Surface polaritons can provide ultra-compacted modes when hybridized, and the modal area can be defined using energy density:

$$A_m = \frac{\iint W(\boldsymbol{r})dxdy}{\max\{W(\boldsymbol{r})\}}, \tag{4}$$

where, in the case of uniaxial material, i.e. 4H-SiC[10],:

$$W(\boldsymbol{r}) = \frac{1}{2}\left[\frac{d(\varepsilon_{\perp}(\omega)\omega)}{d\omega}|E_x|^2 + \frac{d(\varepsilon_{\parallel}(\omega)\omega)}{d\omega}|E_y|^2 + \frac{d(\varepsilon_{\perp}(\omega)\omega)}{d\omega}|E_z|^2 + \mu_0|H(\boldsymbol{r})|^2\right]. \tag{5}$$

Modal area is typically normalized to the diffraction-limited area in free space: $A_0 = \lambda_0^2/4$. Ansys high frequency structural simulator (HFSS) is a commercial finite element method (FEM) solver where driven HFSS models were employed to characterize the hybrid waveguide shown in Figure 1 and the optical directional coupler (ODC) and Mach-Zehnder interferometer (MZI) in the following sections. Table 1 tabulates the numerical results for effective hybrid index, propagation length, normalized modal area, and modal character for the hybrid waveguide employed in designing the ODC and MZI.

Table 1. The HFSS driven model analysis for the hybrid SPhP enhanced waveguide shown in Figure1.

| $\mathbf{n_{hyb}}$ | $\mathbf{L_m}$ **[µm]** | $\mathbf{A_m/A_0}$ | $\boldsymbol{|a|^2}$ |
|---|---|---|---|
| 1.62 | 49.0 | 1.57E-2 | 55.8% |

This endeavor reports on first numerical results, to the best of the authors' knowledge, of optical directional coupler and Mach-Zehnder interferometer using a hybrid SPhP waveguide in the mid to long IR spectrum.ODC and MZI are elementary devices that can enable technology in applications like quantum information, photonic integrated circuits (PIC), and IR sensingtechnology[11-15].

## 2. OPTICAL DIRECTIONAL COUPLER DESIGN

An ODC is a two-input-two-output optical device with isolated input and outputs ports. In the center is a coupling region that allows the transfer of power between the branches as a function of coupling length "L". Four s-bend waveguides formed out of the A-Si traces are used to create the ODC. To aid in design of the ODC, two lines where investigated for coupling and isolation from each other as shown in Figure 2.As it can be seen from Figure 2, under3% of the power is coupled into the other line with separation "s" that is greater than 4 µm therefore; to provide isolation of the input and output the ports are separated by a distance greater than 4 µm as can be seen in Figure 3.

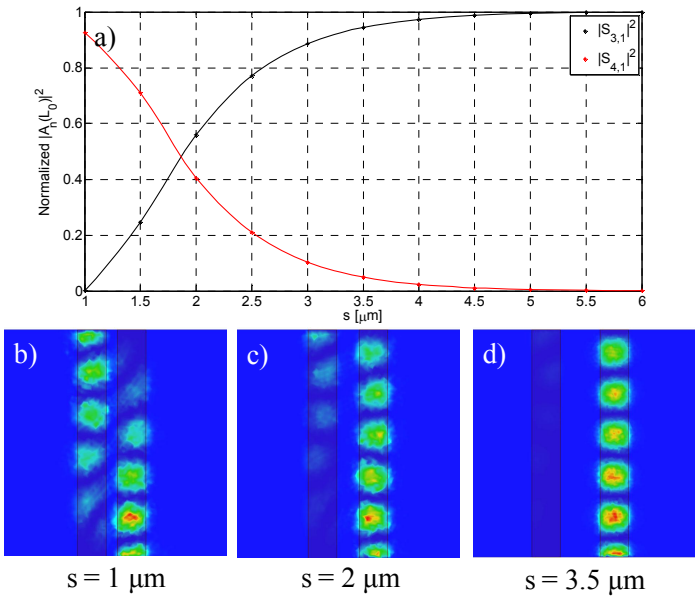


Figure 2. a) The normalized power for both output ports 3 and 4 as a function of waveguide separation "s" is shown. The $|E|^2$ on the 4H-SiC/GaN interfaces is show for s equal to 1μm (b), 2 μm (c), and 3.5 μm (d).

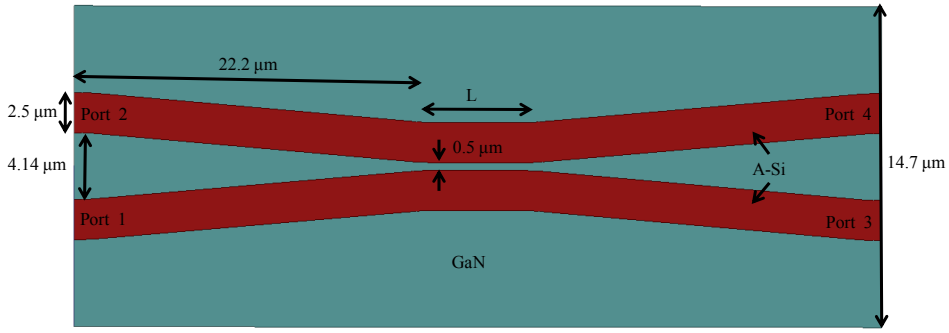


Figure 3. ODC top view under consideration with dimension labeled.

The output power for a phased matched or symmetrical ODC is governed by[7,16]:

$$|A_1(z)|^2 = e^{-2\alpha L}\cos^2\left(\frac{\pi}{2L_0}L\right), \tag{6.a}$$

$$|A_2(z)|^2 = e^{-2\alpha L}\sin^2\left(\frac{\pi}{2L_0}L\right), \tag{6.b}$$

where $L_0$is the transfer length (or $2L_0$is called the beat length) and α is the field attenuation due to propagation losses. The transfer length is the coupling length needed to couple the output power from one waveguide into another. Figure 4.a show the sinusoidal dependence of port output power with coupling distance as determined by eq. 6.For this particular design the transfer length is 14.1 μm which can be seen in Figure 4.a.The phase difference between the output ports can be seen in part b of Figure 4. Given that ellipsometry-measured material properties[17]are imported into HFSS, the variation off of the $\pm 90^0$in the phase difference is a results of the lossy nature and internal damping of the materials in particular the polar dielectric, 4H-SiC, that is used. The $|E|^2$at the 4H-SiC/GaN interfaces at approximately 3dB splitter is shown in Figure 4.c.It can be seen from the $|E|^2$ of the 3dB splitter in Figure 4.c, due to the gradual bend of the s-bend the transfer of the field from waveguide one into two occurs within the bend.

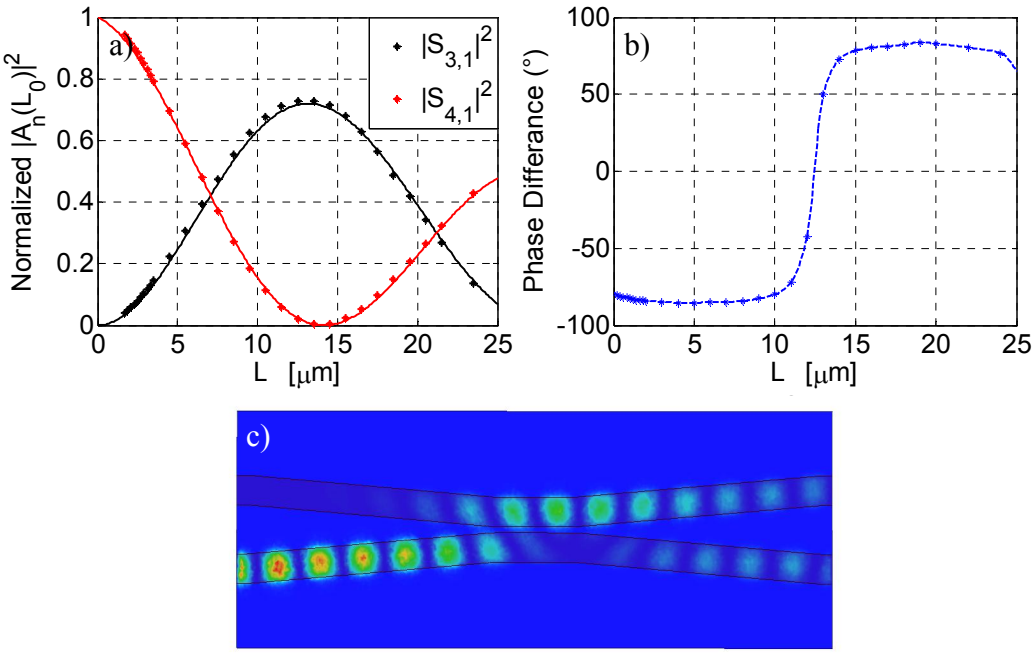


Figure 4. The normalized power a) and phase difference between the ports b) of the output ports at varies coupling lengths. c) The $|E|^2$ at the 4H-SiC/GaN interfaces is shown for when the ODC is a 3dB splitter.

## 3. MACH-ZEHNDER INTERFEROMETER DESIGN

Next, a MZI is designed and characterized numerically using HFSS. Two ODCs are combined with a 5.0 μm straight waveguide sections connecting the two ODC as seen in Figure 5. Similar as in the case of the ODC, the coupling region of the two ODCs were tuned simultaneously with the same length. The resulting normalized output power is shown in Figure 6.a as a function of coupling length. As before in the ODC case, an exponentially decaying sinusoidal fit was used as seen in Figure 6.a. Figure 6.b shows the $|E|^2$ at the 4H-SiC/GaN interfaces for when the coupling length is at the 3dB splitter/combiner point.

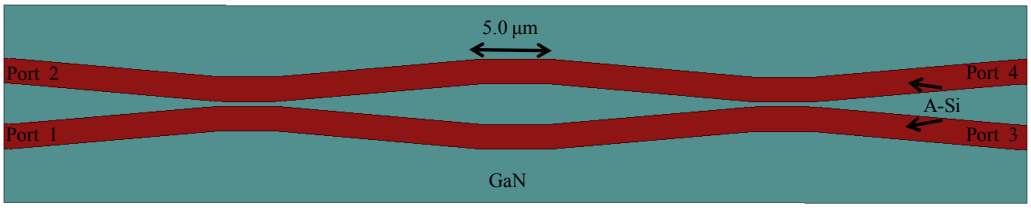


Figure 5. The top view of the MZI under consideration is shown.

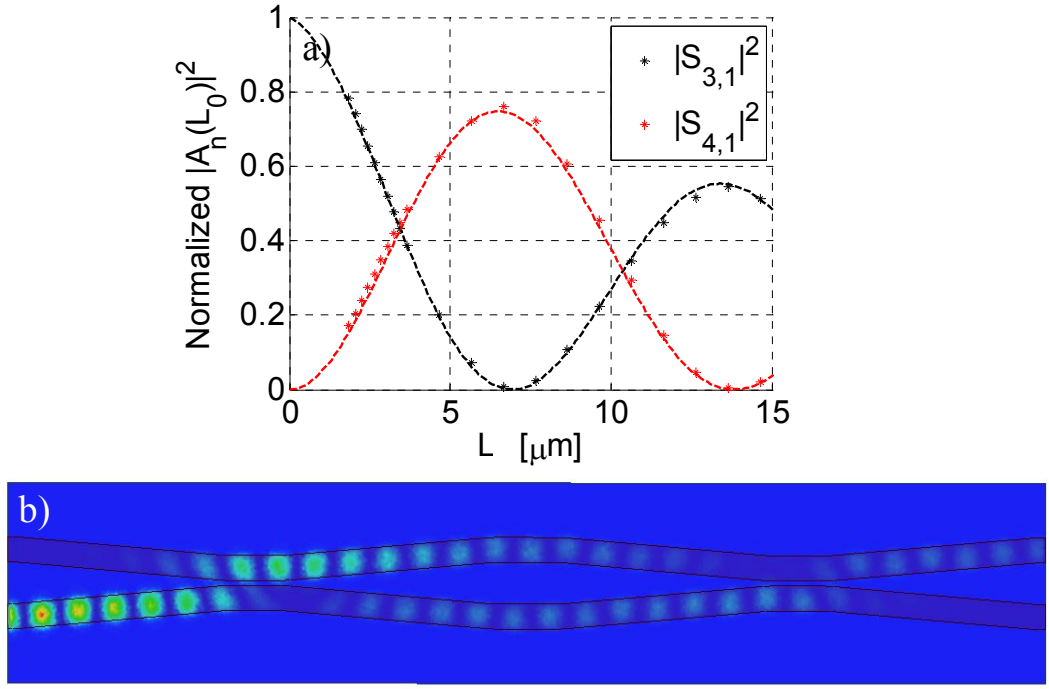


Figure 6. a) The normalized output port power is shown as a function of coupling length of the ODC. b) The $|E|^2$ at the 4H-SiC/GaN interfaces is shown for when the ODC coupling length are at 3dB splitter/combiner.

## 4. CONCLUSION

In conclusion, a hybrid SPhP enhanced waveguide was implemented in the design of an ODC and MZI using FEM solver HFSS. Both devices, ODC and MZI, have a transverse size smaller than the free space wavelength of approximately 9.25 μm. Due to nature of the surface polaritons, subwavelength or ultra-compactness transverse size ODC and/or MZI are potentially achievable by decreasing the modal area of the initial hybrid waveguide however; at a cost of the propagation length[1,5].With the MZI device length on the order of 100 μm, a reduction of propagation length would not be appealing given the propagation length tabulated in Table 1.Alternatively,a reduction of the transverse separation between the inputs could be traded-off for a reduction in isolation to reduce transverse size. Future work will include investigating using other hybrid waveguide design, in particular that use of equivocated polar dielectric metal-isolator-metal (MIM) or isolator-metal-isolator (IMI) heterostructure[2]. Also, the concept of hybrid materials where polar dielectrics couple with graphene[18,19] resulting in a material gains attributed of the un-joined material[20-22]. In particular, hybrid material retain graphene electrooptic properties[20,21] make it possible for ultra-compact optical switches and modulators in the mid to long IR with the used of surface polaritons[19,23].

## REFERENCES


[1] R. F. Oulton, V. J. Sorger, D. A. Genov, D. F. P. Pile, and X. Zhang, "A hybrid plasmonic waveguide for subwavelength confinement and long-range propagation," *Nature Photonics*, vol. 2, pp. 496-500, August 2008.

[2] Z. Han, L. Liu, and E. Forsberg, "Ultra-compact directional couplers and Mach-Zehnder interferometers employing surface plasmon polaritons," *Optics Communications*, vol. 259, no. 2, pp. 690-695, March 2006.

[3] J. D. Caldwell et al., "Low-loss, infrared and terahertz nanophotonics using surface phonon polaritons," *Nanophotonics*, vol. 4, no. 1, pp. 44-48, January 2015.

[4] J. D. Caldwell et al., "Sub-diffraction, volume-confined polaritons in the natural hyperbolic material, hexagonal boron nitride," *Nature Communications*, vol. 5, no. 5221, pp. 1-9, October 2014.

[5] M. F. Finch, C. A. B. Saunder Filho, N. Premkumar, Y. Yang, and B. A. Lail, "A 4H-SIC Phonon Polariton Enhanced Hybrid Waveguide," in *2016 IEEE International Symposium an Antennas and Propagation and USNC-URSI Radio Science Meeting*, Fajardo, Puerto Rico, 2016, pp. 1-2.

[6] Y. Yang, F. M. Manene, and B. A. Lail, "Infrared surface phonon polariton waveguides on SiC substrate," *Proceedings SPIE 9547, Plasmonics: Metallic Nanostructures and Their Optical Properties XIII*, vol. 9547, no. 954723, pp. 1-7, August 2015.

[7] B. E. A. Saleh and M. C. Teich, "Guided-wave Optics," in *Fundamentals of Photonics*, J. W. Goodman, Ed. New York, United States of America: John Wiley & Sons, Inc., 1991, ch. 7, pp. 238-271.

[8] H. A. Haus, *Waves and Fields in Optoelectronics*. Englewood Cliffs, NJ: Prentice-Hall, Inc., 1984.

[9] Hermann A. Haus and Weiping Huang, "Coupled-Mode Theory," *Proceeding of the IEEE*, vol. 79, no. 10, pp. 1505-1518, 1991.

[10] T. E. Tiwald, J. A. Woollam, S. Zollner, J. Christiansen, and R. B. Gregory, "Carrier concentration and lattice absorption in bulk and epitaxial silicon carbide determined using infrared ellipsometry," *Physical Review B*, vol. 60, no. 16, pp. 464-474, October 1999.

[11] Y. Fang and M. Sun, "Nanoplasmonic waveguides: towards applications in integrated nanophotonic circuits," *Light: Science & Applications* , vol. 4, no. e294, pp. 1-11, February 2015.

[12] V. J. Sorger, R. F. Oulton, R. Ma, and X. Zhang, "Toward integrated plasmonic circuits," *Materials Research Society Bulletin*, vol. 37, no. 08, pp. 728-738, August 2012.

[13] V. M. N. Passaro, F. Dell'Olio, C. Ciminelli, and M. N. Armenise, "Efficient chemical sensing by coupled slot SOI waveguides ," *Sensors*, vol. 9, no. 2, pp. 1012-1032, February 2009.

[14] D. K. Gramotnev and S. I. Bozhevolnyi, "Plasmonics beyond the diffraction limit," *Nature Photonics*, vol. 4, pp. 83-91, January 2010.

[15] F. Lou, Z. Wang, D. Dai, L. Thylen, and L. Wosinski, "Experimental demonsration of ultra-compact directional couplers based on silicon hybrid plasmonic waveguides," *Applied Physics Letters*, vol. 100, no. 241105, pp. 1-4, June 2012.

[16] R. G. Hunsperger, "Coupling Between Waveguides," in *Integrated Optics: Theory and Technology*. New York, United States of America: Springer, 2009, ch. 8, pp. 153-169.

[17] J. Ginn et al., "Characterizing Infrared Frequency Selective Surfaces on Dispersive Media," *ACES Journal* , vol. 22, no. 1, pp. 184-188, March 2007.

[18] A. Vakil and N. Engheta, "Transformation optics using graphene," *Science*, vol. 332, no. 6035, pp. 1291-1294, June 2011.

[19] S. He, X. Zhang, and Y. He, "Graphene nano-ribbon waveguides of record-small mode area and ultra-high effective refractive indices for future VLSI," *Optics Express*, vol. 21, no. 25, pp. 30664-30673, December 2013.

[20] J. D. Caldwell et al., "Atomic-scale photonic hybrids for mid-infrared and terahertz nanophotonics," *Nature nanotechnology*, vol. 11, no. 1, pp. 9-15, January 2016.

[21] S. Dai et al., "Graphene on hexagonal boron nitride as a tunable hyperbolic metamaterial," *Nature Nanotechnology*, vol. 10, no. 8, pp. 682-686, June 2015.

[22] Z. Fei et al., "Infrared nanoscopy of dirac plasmons at the graphene-SiO2 interface," *Nano Letter*, vol. 11, no. 11, pp. 4701-4705, October 2011.

[23] J-S. Shin, J-S. Kim, and J. T. Kim, "Graphene-based hybrid plasmonic modulator," *Journal of Optics*, vol. 17, no. 12, p. 125801, October 2015.